

# Control Reconfiguration to Improve HDA Process Optimality<sup>\*</sup>

Lingjian Ye<sup>\*</sup> Martyna Królicka<sup>\*\*</sup> Yi Cao<sup>\*\*\*</sup>

<sup>\*</sup> Ningbo Institute of Technology, Zhejiang University, 315100, Ningbo,  
China (e-mail: lingjian.ye@gmail.com)

<sup>\*\*</sup> School of Water, Energy and Environment, Cranfield University,  
Cranfield, Bedford MK43 0AL, UK (e-mail:  
Martyna.Krolicka@cranfield.ac.uk, y.cao@cranfield.ac.uk)

<sup>\*\*\*</sup> College of Chemical and Biological Engineering, Zhejiang  
University, 310027, Hangzhou, China (e-mail: yi4cao2@gmail.com)

**Abstract:** Control structure design for the large-scale hydrodealkylation of toluene (HDA) process has been extensively studied. The systematic procedure based on self-optimizing control was successfully applied to the HDA process with a promising control configuration. Besides of the active constraints identified, the remaining self-optimizing controlled variables are selected as the mixer outlet methane mole fraction and the quencher outlet toluene mole fraction, which are nonetheless single measurements. In this paper, we consider control reconfiguration for the HDA process by selecting measurement combinations as CVs to improve the process optimality. To this end, the recently proposed global self-optimizing control (gSOC) approach is employed for CV selection and the partial bidirectional branch and bound algorithm ( $PB^3$ ) is used for fast-screening measurement candidates. Numerical controlled variables are derived and the economic optimality is improved by the reconfiguration.

*Keywords:* HDA process, control configuration, self-optimizing control, plant-wide control

## 1. INTRODUCTION

Due to the competitive market, industrial processes have to be continuously operated in an optimal manner. Control system configurations have a significant influence on the optimality of process operation. To ensure the optimality persistent, sometimes, a reconfiguration is desirable due to changes in operational objectives and conditions, or newly developed more advanced techniques, which make the existing control configuration not optimal anymore.

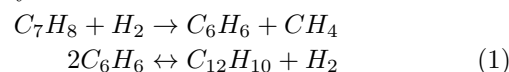
Self-optimizing control (SOC) is a control configuration method (Skogestad, 2000; Jäschke et al., 2017) to select a set of controlled variables so that when these variables are perfectly controlled, the overall operation is optimal or near optimal. Due to the difficulty to solve such a problem, initial solutions of SOC have to rely on linearized models, hence were only locally valid (Alstad and Skogestad, 2007; Kariwala et al., 2008). Recently, the concept of global SOC (gSOC) has been proposed (Ye and Cao, 2012; Ye et al., 2013, 2014, 2015) to improve SOC performance in a larger operating window. The gSOC technique has been applied to the large-scale Tennessee Eastman process to retrofit existing control configurations by introducing a new SOC layer to update set points of the existing control loops (Ye et al., 2017) resulting in significantly improved optimality.

In this work, the concept of gSOC is further applied to control reconfiguration of the the hydrodealkylation of toluene (HDA) process (Douglas, 1988). Control configurations for the HDA process have been extensively studied in the literature, *e.g.* in early works by Cao (1995); Cao and Biss (1997); Cao et al. (1998) and plant-wide process control (Luyben et al., 1999). More recently, for economically optimal operation, de Araujo et al. (2007a,b) systematically studied the HDA process and concluded a self-optimizing control configuration based on local SOC approaches. As the SOC theory has been advanced to gSOC, it is now possible to carry out control reconfigurations using the new tools, such that the process optimality can be further improved.

The paper is organised as follows, after an overview of the HDA process in section 2, the systematic approach for control configuration of the HDA process is illustrated in section 3. Then, the new gSOC reconfiguration is presented in section 4 with improved performance demonstrated in section 5. Finally, the work is concluded in section 6.

## 2. OVERVIEW OF HDA PROCESS

The HDA process produces high purity benzene through the hydrodealkylation of toluene. Two main reactions are



In the HDA plant, two input streams are fed at 550 psia and 38°C, one of which is fresh toluene and the other is a mixture of 97% hydrogen and 3% methane. Methane

<sup>\*</sup> The author Lingjian Ye gratefully acknowledge the National Natural Science Foundation of China (NSFC) (61673349, 61304081), Ningbo Natural Science Foundation (2015A610151), Talent project of Zhejiang Association of Science and Technology (2017YCGC014).

is an undesired byproduct and must be removed through a purge to prevent a damage to the process. Unreacted hydrogen is recycled to reduce raw material cost.

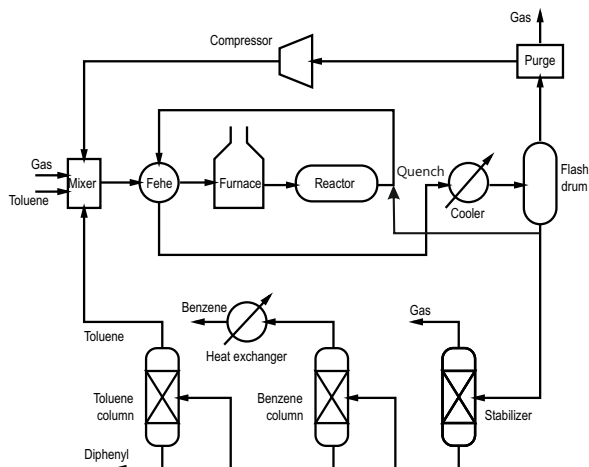


Fig. 1. The HDA plant

The flowsheet of the HDA plant is shown in Figure 1, where the mixture of toluene and hydrogen from two inlet feeds and two recycled flows is preheated in a feed-effluent heat exchanger (FEHE) by the reactor outflowing stream. The mixed stream is further heated in a furnace before being fed to an adiabatic plug-flow reactor. The reactor outlet stream is then quenched to 621°C by the liquid flow from the flash drum to prevent coking. The temperature of the effluent is further reduced through the FEHE and a cooler before it is flashed into a vapor and a liquid streams. The unreacted hydrogen and methane in the vapor phase are compressed and recycled back, some of which are purged from the system. The liquid stream leaving the flasher enters into a chain of three distillation columns. The first one, stabilizer, removes hydrogen and methane in the overhead. The bottom product is fed into the second benzene column, which delivers the benzene as distillate. The last toluene column separates the unconverted toluene (top) and diphenyl (bottom). The toluene is recycled into the mixer to combine the inlet feeds.

*Manipulated variables and measurements.* Total 21 manipulated variables (MVs) and 140 measurements are defined in the HDA model. Descriptions are given in Table 1 and 2, respectively. The measurements are more complete than de Araujo et al. (2007a), where only 70 are considered.

*Constraints.* Important process constraints are defined in Table 3. These constraints are to ensure the process safety, production health, equipment capacity, and so on.

*Operational objective.* The profit function ( $-J$ [M\$/year]) to be maximized is defined as follows

$$-J = (p_{ben}D_{ben} + p_{fuel}Q_{fuel}) - (p_{tol}F_{tol} + p_{gas}F_{gas} + p_{fuel}Q_{fuel} + p_{cw}Q_{cw} + p_{pow}W_{pow} + p_{stm}Q_{stm}) \quad (2)$$

where  $D_{ben}$ ,  $F_{tol}$ ,  $F_{gas}$ ,  $W_{comp}$  and  $Q_{fuel}$  are flowrates of benzene, toluene, hydrogen, compressor power and fuel to the furnace.  $Q_{cw}$  is the summation of water delivered to cooler, stabilizer, benzene and toluene columns.  $Q_{stm}$  denotes steam of stabilizer, benzene and toluene column.  $p$ . is the price of associated quantity.

Table 1. Manipulated variables

Number	Variable name
U1	Fresh gas feed rate
U2	Furnace outlet temperature (set point)
U3	Purge valve upstream pressure
U4	Cooler outlet temperature (set point)
U5	Fresh toluene feed rate
U6	Bypass ratio
U7	Compressor power
U8	Stabilizer top light key recovery (methane)
U9	Stabilizer top heavy key recovery (benzene)
U10	Benzene column bottom light key recovery (benzene)
U11	Benzene column bottom heavy key recovery (toluene)
U12	Toluene column top light key recovery (toluene)
U13	Toluene column top heavy key recovery (diphenyl)
U14	Flow of cooling stream to quencher
U15	Liquid flow to stabilizer
U16	Stabilizer distillate rate
U17	Stabilizer bottoms rate
U18	Benzene column distillate rate
U19	Benzene column bottoms rate
U20	Toluene column distillate rate
U21	Benzene column bottoms rate

Table 2. Measurements

Number	Variable
Y1	Mixer outlet temperature
Y2	FEHE hot side outlet temperature
Y3	Cooler inlet temperature
Y4	Furnace inlet temperature
Y5	Furnace outlet temperature
Y6–Y24	Reactor section 1–19 temperature
Y25	Quencher outlet temperature
Y26	'Separator temperature'
Y27–Y28	Compressor inlet and outlet temperature
Y29–Y49	Flowrates of fresh toluene, gas, mixer outlet, quencher outlet, FEHE hot side outlet, separator vapor outlet, separator liquid outlet, purge, Compressor inlet, Stabilizer boilup, Benzene column boilup, Toluene column boilup, Stabilizer reflux, Benzene column reflux, Toluene column reflux, Stabilizer bottom, Benzene column bottom, Toluene column bottom, Stabilizer distillate, Benzene column distillate, Toluene column distillate
Y50–Y54	Mixer outlet mole fraction of hydrogen, methane, benzene, toluene, diphenyl
Y55–Y59	Quencher outlet mole fraction of hydrogen, methane, benzene, toluene, diphenyl
Y60–Y64	Separator overhead vapor outlet mole fraction of hydrogen, methane, benzene, toluene, diphenyl
Y65–Y69	Separator liquid outlet mole fraction of hydrogen, methane, benzene, toluene, diphenyl
Y70–Y74	Stabilizer bottom mole fraction of hydrogen, methane, benzene, toluene, diphenyl
Y75–Y79	Benzene bottom mole fraction of hydrogen, methane, benzene, toluene, diphenyl
Y80–Y84	Toluene bottom mole fraction of hydrogen, methane, benzene, toluene, diphenyl
Y85–Y89	Stabilizer distillate mole fraction of hydrogen, methane, benzene, toluene, diphenyl
Y90–Y94	Benzene distillate mole fraction of hydrogen, methane, benzene, toluene, diphenyl
Y95–Y99	Toluene column distillate mole fraction of hydrogen, methane, benzene, toluene, diphenyl
Y100–Y110	Pressure of mixer outlet, FEHE hot side outlet, cooler inlet & outlet, furnace inlet & outlet, reactor outlet, separator, Separator overhead vapor, compressor inlet & outlet
Y111–Y118	Heat duty of furnace, cooler, stabilizer reboiler and condenser, benzene column reboiler and condenser, toluene column reboiler and condenser
Y119–Y124	Stabilizer bottoms and distillate, Benzene column bottoms and distillate, Toluene column bottoms and distillate, to feed flow ratio
Y125	Compressor power
Y126	Flow through bypass around FEHE
Y127	Purge control setpoint pressure
Y128	Hydrogen to aromatics ration in reactor inlet
Y129	Toluene conversion at reactor outlet
Y130	Flow of cooling stream to quencher
Y131	Stabilizer bottoms hydrogen + methane mole fraction
Y132–Y134	Openings of separator inlet, vapor and liquid valves
Y135–Y136	Key recovery in stabilizer top: methane and benzene
Y137–Y138	Key recovery in benzene column bottom: benzene & toluene
Y139–Y140	Key recovery in toluene column top: toluene & diphenyl

Table 3. Process constraints

Constraints
1. Production rate $\geq 265$ lb mol/h
2. Hydrogen to aromatic ratio in reactor inlet $\geq 5$
3. Maximum toluene feed rate $\leq 300$ lb mol/h
4. Reactor inlet pressure $\leq 500$ psia
5. Reactor outlet temperature $\leq 1300^\circ F$
6. Quencher outlet temperature $Y \leq 1150^\circ F$
7. Product purity at the benzene column distillate $\geq 0.9997$
8. Separator inlet temperature $\geq 95^\circ F$ and $\leq 105^\circ F$
9. Reactor inlet temperature $\geq 1150^\circ F$
10. Non-negative flows and concentrations

Table 4. Disturbances

	Nominal	Change
D1 Fresh toluene feed rate (lb mol/h)	300	285
D2 Fresh toluene feed rate (lb mol/h)	300	315
D3 Fresh gas feed rate methane mole fraction	0.03	0.08
D4 Hydrogen to aromatic ratio in reactor inlet	5.0	5.5
D5 Reactor inlet pressure (psi)	500	520
D6 Quencher outlet temperature ( $^\circ F$ )	1150	1170
D7 Product purity in benzene column distillate	0.9997	0.9960

*Disturbances.* In this paper, the seven disturbances shown in Table 4 are considered. Disturbances 8–12 defined in (de Araujo et al., 2007a) are not included as they impose minor steady state effects.

The operation objective for the HDA plant can be summarized as maximizing the process profit (2) under different disturbances (Table 4), while ensuring all constraints satisfied (Table 3). This goal is greatly influenced by the configuration of control structure.

### 3. EXISTING CONTROL CONFIGURATION

#### 3.1 Brief description

The existing control configuration was derived based on the systematic procedure by Skogestad (2004) to design complete control structures for large-scale chemical plants to be “self-optimizing”, by means of selecting controlled variables (CVs) from an economic perspective.

In summary, the whole procedure consists of the following steps: (1) Top-down design: 1.1 defining operational objective; 1.2 degree of freedom analysis; 1.3 selecting primary CVs; 1.4 set production rate; (2) Bottom-up design for the regulatory control layer, 2.1 stabilization; 2.2 local disturbance design; (3) Supervisory control layer: determine centralized or decentralized control; (4) Optimization layer (may unnecessary); (5) Validations. Among these steps, the top-down design is mainly concerned with the economic optimality, whereas the bottom-up design deals with controllability and stability.

It has been recognized that the primary CVs are the most important for steady state economics, which is particularly highlighted in the self-optimizing control (Skogestad, 2000). To select CVs, suppose that the operational objective is formulated as the following optimization problem

$$\min_{\mathbf{u}} J(\mathbf{u}, \mathbf{d}), \quad s.t. \quad \mathbf{g}(\mathbf{u}, \mathbf{d}) \leq 0 \quad (3)$$

with the measurement mapping as

$$\mathbf{y} = \mathbf{f}(\mathbf{u}, \mathbf{d}) \quad (4)$$

where  $J$  is the cost function to be minimized,  $\mathbf{u} \in \mathbb{R}^{n_u}$ ,  $\mathbf{d} \in \mathbb{R}^{n_d}$ , and  $\mathbf{y} \in \mathbb{R}^{n_y}$  are the manipulated variables (MVs), disturbances, and measurements, respectively.  $\mathbf{f} : \mathbb{R}^{n_u \times n_d} \rightarrow \mathbb{R}^{n_y}$  is the measurement model.

Besides of the level control which has no steady state effects, the primary CVs are denoted as  $c_1 = [c_a \ c]^T$ , where  $c_a$  is the active constraints (a subset of  $g$ ) and  $c$  is the CVs associated with the unconstrained part. Without loss of generality, assume that  $c_a$  has been controlled with appropriate MVs and perfectly controlled, an unconstrained optimization problem can be derived

$$\min_{\mathbf{u}} J(\mathbf{u}, \mathbf{d}) \quad (5)$$

where the same symbol  $u$  is used to denote the remaining MVs for simplicity. To evaluate, the economic loss is defined as

$$L = J(\mathbf{u}, \mathbf{d}) - J^{\text{opt}}(\mathbf{d}) \quad (6)$$

where  $J^{\text{opt}}(\mathbf{d})$  is the true minimal cost when disturbances occur. Originally, the unconstrained CVs  $c$  are selected as follows (Skogestad, 2000)

- (1) Identify all possible disturbances;
- (2) Select a measurement set as CV candidates, say  $c \in \{y\}$ ;
- (3) For all possible  $c \in \{y\}$ , evaluate the close-loop loss  $L$  for all disturbance scenarios;
- (4) Select promising CV candidates with least losses for further evaluations, e.g. the dynamic validations.

In the above steps for selecting CVs, Step (3) is a main time-consuming step which may lead to the computation intractable for large-scale processes. Faster (but less rigorous) algorithms have been considered to evaluate the loss in Step (3) (Halvorsen et al., 2003). For example, in the local analysis it was proposed to minimize  $\underline{\sigma}(S_1 G J_{uu}^{-1/2})$  or  $\underline{\sigma}(S_1 G)$  ( $S_1$  is a scale matrix,  $G$  is the gain matrix and  $J_{uu}$  is the cost Hessian,  $\underline{\sigma}(\cdot)$  stands for the minimal singular value of a matrix). The latter is referred as the minimum singular value rule in Halvorsen et al. (2003).

#### 3.2 CV selection results for HDA process

The above systematic procedure has been applied to the HDA process. The results of selected CVs in the following are summarized from de Araujo et al. (2007a).

Among 21 dynamic DOFs, 7 is first consumed to control liquid levels that have no steady state effects. The bypass ratio is often fixed at 1. Furthermore, 11 active constraints are identified by optimization of either the three columns or the entire process (de Araujo et al., 2007a), as given in Table 5. These active constraints should be controlled for all disturbances to improve the process optimality.

Therefore, there are only 13-11=2 DOFs left. By eliminating those measurements already been controlled, there are still substantial candidates which give numerous possibilities. Since rigorous evaluation for the close-loop loss would be difficult, the local criterions of  $\underline{\sigma}(S_1 G J_{uu}^{-1/2})$  and  $\underline{\sigma}(S_1 G)$  are used by de Araujo et al. (2007a) as an alternative. Table 6 shows the most 5 promising subsets for CVs, all of which contain the mixer outlet methane mole fraction. Controlling the mixer outlet methane mole fraction and quencher outlet toluene mole fraction leads to the least economic loss, averagely 15.39 k\$/year in their study de Araujo et al. (2007a).

Table 5. Active constraints for the HDA process

Variable	value	bound type
Quencher outlet temperature	1150 °F	upper bound
Separator temperature	95 °F	lower bound
Fresh toluene feed flow rate	300 lb mol/h	upper bound
Reactor inlet pressure	500 psia	upper bound
Hydrogen to aromatic ratio in reactor inlet	5	upper bound
Benzene mole fraction in stabilizer distillate	0.0001	specification <sup>a</sup>
Methane mole fraction in stabilizer bottoms	0.000001	specification <sup>a</sup>
Benzene mole fraction in benzene column distillate	0.9997	lower bound
Benzene mole fraction in benzene column bottoms	0.0013	specification <sup>a</sup>
Diphenyl mole fraction in toluene column distillate	0.0005	specification <sup>a</sup>
Toluene mole fraction in toluene column bottoms	0.0004	specification <sup>a</sup>

<sup>a</sup>identified by optimization of the three columns, where the variables lie in “flat” regions for the economic effect

Table 6. Promising CVs selected by de Araujo et al. (2007a)

Rank	subsets	average loss (k\$/year)
1	Y51, Y58	15.39
2	Y51, Y129	26.55
3	Y51, Y67	31.39
4	Y51, Y68	40.40
5	Y51, Y62	51.75

#### 4. GSOC AND PB<sup>3</sup> FOR CV SELECTION

Methodologies in this section are to improve the self-optimizing performance by reconfiguring the large-scale HDA process, where the gSOC approach selects measurement combinations as CVs and the PB<sup>3</sup> algorithm fast identifies promising measurement subsets. Recently, the integration of these two methodologies has successfully retrofitted the control configuration of Tennessee Eastman process (Ye et al., 2016, 2017).

##### 4.1 Global self-optimizing control

Firstly, the economic loss is approximated by a quadratic function as

$$L = \frac{1}{2} \mathbf{e}_c^T \mathbf{J}_{cc} \mathbf{e}_c \quad (7)$$

where  $\mathbf{e}_c \triangleq \mathbf{c} - \mathbf{c}^{\text{opt}}$  is the deviation of  $\mathbf{c}$  from its optimal value  $\mathbf{c}^{\text{opt}}$ ,  $\mathbf{J}_{cc}$  is the Hessian of  $J$  with respect to  $\mathbf{c}$  at the optimal point, which can be evaluated as  $\mathbf{J}_{cc} = (\mathbf{H}\mathbf{G}_y)^{-T} \mathbf{J}_{uu} (\mathbf{H}\mathbf{G}_y)^{-1}$  ( $\mathbf{G}_y$  and  $\mathbf{J}_{uu}$  are the sensitivity matrix of  $\mathbf{y}$  and Hessian of  $J$  respectively, both with respect to  $\mathbf{u}$ ). Since at the optimum,  $\mathbf{c}^{\text{opt}} = \mathbf{H}\mathbf{y}^{\text{opt}}$  and considering that the measured CVs,  $\mathbf{c}_m$  are controlled as  $\mathbf{c}_m = \mathbf{H}\mathbf{y}_m = \mathbf{c}_s = 0$ , the true value of  $\mathbf{c}$  is  $\mathbf{c} = \mathbf{c}_m - \mathbf{H}\mathbf{n} = -\mathbf{H}\mathbf{n}$ . Therefore,  $\mathbf{e}_c = -\mathbf{H}(\mathbf{y}^{\text{opt}} + \mathbf{n})$ . Notice that, we consider introducing the general CVs,  $\hat{\mathbf{c}} \triangleq \mathbf{c} - \mathbf{c}_s$ , which should be controlled at zero. The optimal value of  $\mathbf{c}_s$  can then be obtained together with  $\mathbf{c}$  by expanding measurements  $\mathbf{y}$  with an artificial measurement (vector  $\mathbf{1}$ ), i.e.  $\hat{\mathbf{y}} = [\mathbf{1} \ \mathbf{y}^T]^T$ . For simplifying notation, in the

remaining part of the paper,  $\mathbf{c}$  and  $\mathbf{y}$  will be used to representing  $\hat{\mathbf{c}}$  and  $\hat{\mathbf{y}}$ , respectively.

By introducing matrices  $\mathbf{Y}$  and  $\tilde{\mathbf{Y}}$  as

$$\mathbf{Y} = [\mathbf{y}_{(1)}^{\text{opt}} \ \cdots \ \mathbf{y}_{(N)}^{\text{opt}}]^T, \quad \tilde{\mathbf{Y}} = \begin{bmatrix} \mathbf{1} \\ \sqrt{N} \mathbf{Y} \end{bmatrix} \quad (8)$$

where  $N$  is the number of sampled disturbances scenarios,  $\mathbf{y}_{(i)}^{\text{opt}}$  denotes the optimal measurement vector and  $\mathbf{W}_n$  is a diagonal matrix with its diagonal elements as the error magnitudes of each measurement. The global optimal CV selection problem can be formulated as

$$\min_{\mathbf{H}} L_{\text{av}} = \frac{1}{2} \|\tilde{\mathbf{Y}}\mathbf{H}^T\|_{\text{F}}^2, \quad \text{s.t. } \mathbf{H}\mathbf{G}_{y,\text{ref}} = \mathbf{J}_{uu,\text{ref}}^{1/2} \quad (9)$$

where the subscript  $(\cdot)_{\text{ref}}$  denotes a chosen reference operating point. This problem is convex and an analytical solution follows in the same form as in local SOC methods

$$\mathbf{H}^T = (\tilde{\mathbf{Y}}^T \tilde{\mathbf{Y}})^{-1} \mathbf{G}_{y,\text{ref}}^T (\mathbf{G}_{y,\text{ref}}^T (\tilde{\mathbf{Y}}^T \tilde{\mathbf{Y}})^{-1} \mathbf{G}_{y,\text{ref}})^{-1} \mathbf{J}_{uu,\text{ref}}^{1/2} \quad (10)$$

See (Ye et al., 2015) for theoretical derivations.

A summary of the gSOC algorithm is given in the following:

- (1) For all  $N$  operating conditions, the cost function  $J$  is minimized and the optimal measurements,  $\mathbf{y}_{(i)}^{\text{opt}}$  are obtained.
- (2) Construct  $\mathbf{Y}$  and  $\tilde{\mathbf{Y}}$  according to eq (8).
- (3) Choose a particular operating point as the reference point, the gain matrix of  $\mathbf{y}$  with respect to the MVs is evaluated as  $\mathbf{G}_{y,\text{ref}}$ .
- (4) The optimal  $\mathbf{H}$  minimizing  $L_{\text{av}}$  is solved as (10).

##### 4.2 PB<sup>3</sup> algorithm

In a large-wide scale problem, there are substantial measurements which are not unnecessarily used for the CVs. However, the subset selection problem is combinatorial in nature and may be computationally intractable to search exhaustively. To this end, a series of bidirectional branch and bound algorithms have been developed for fast measurement selection (Cao and Kariwala, 2008; Kariwala and Cao, 2009, 2010). In the bidirectional branch and bound algorithms, candidate measurement subsets are divided into branches and evaluated based on the upwards and downwards pruning criteria. Branches, which satisfy either upwards or downwards pruning criteria will be fixed or removed from candidate list, respectively. This way, most non-optimal candidate subsets can be eliminated without further evaluations. The optimal subset is then efficiently identified.

Recently, the widely used PB<sup>3</sup> algorithm based on local SOC criterion (Kariwala and Cao, 2010) has been extended to the global loss criterion (Ye et al., 2017). Basically, the core part of the existing PB<sup>3</sup> algorithm (Kariwala and Cao, 2010) is used to solve the gSOC subset selection problem, however, some modifications are made to prepare appropriate matrices and to ensure constant 1 will always be included. For more detailed descriptions of general principles, as well as discussions on computational complexities of bidirectional branch and bound and the

PB<sup>3</sup> algorithm, readers are referred to Cao and Kariwala (2008); Kariwala and Cao (2009, 2010).

## 5. IMPROVED CONTROL CONFIGURATION

In this section, the control reconfiguration for HDA process will proceed with the same active constraints shown in Table 5, hence only the remaining 2 unconstrained DOFs will be redesigned.

### 5.1 Preparations

For the 2 unconstrained DOFs, without loss of generality, the U2 (Furnace outlet temperature) and U3 (Purge valve upstream pressure) are selected, hence an unconstrained optimization is reformulated. Following the procedure of gSOC, the following steps are in order:

- (1) The nominal operation together with the 7 disturbance scenarios (Table 4) define 8 operating conditions, which are numerically optimized and with the optimal measurements stored. It turns out that among all disturbances, D1 and D2 impose relatively large effects on the optimal profit, where the profit decreases by 6.18 % for D1 and increases by 6.15 % for D2, respectively. On the other hand, D3–D7 impose less than 3% effects on the profit.
- (2) The extended matrix  $\tilde{\mathbf{Y}}$  is constructed based on the optimal measurements. In this paper, we do not include measurement noise. Hence, we set  $\mathbf{W} = \alpha\mathbf{I}$  to avoid the singularity problem, where  $\alpha$  is a very small number.
- (3) Around the optimally nominal point, the gain matrix  $\mathbf{G}_{y,ref}$  and Hessian  $\mathbf{J}_{uu,ref}$  are evaluated using the finite difference method.

$$\mathbf{J}_{uu,ref} = 10^{-4} \times \begin{bmatrix} 1.647 & 1.516 \\ 1.516 & 2.916 \end{bmatrix}$$

and  $\mathbf{G}_{y,ref}$  is not shown due to the space limit.

Theoretically, a combination matrix  $\mathbf{H}$  can be readily solved following the step (5) of gSOC. However, it is clearly unnecessary and complicated to use all measurements (over 100) to constitute the CVs. Hence it is critical to identify promising subsets using the PB<sup>3</sup> algorithm.

### 5.2 CV results with subset selection

Among 140 measurements, 11 variables in the active constraints have been eliminated from the candidate set. Besides, there are many “null” measurements which do not contribute reflecting process information. For example, the toluene mole fraction in the stabilizer distillate is always 0 in the whole operating range. Such measurements are associated with small gains hence can be identified based on the obtained  $\mathbf{G}_{y,ref}$ . To this end, we identify 33 variables whose gain magnitudes in  $\mathbf{G}_{y,ref}$  are less than 0.00005, these variables are eliminated from the candidates.

At this stage, we are left with 92 measurements which can be further used for CV selection and subset identification. The PB<sup>3</sup> algorithm is applied in a PC with Intel i5 @3.3GHz CPU and 16 GB RAM. In general, the algorithm

Table 7. Promising measurement subsets and economic losses

	Measurements	$L_{av}$ [k\$/y]
$n_y=2$	Y32,Y111	2.26
	Y34,Y111	2.41
de Araujo et al. (2007a)	Y51, Y58	5.49
	(nominal setpoints)	5.97
$n_y=3$	Y35,Y53,Y115	0.287
	Y53,Y57,Y115	0.931
	Y3,Y35,Y51	1.03
$n_y=4$	Y2,Y35,Y47,Y115	0.205
	Y37,Y41,Y58,Y115	0.224
$n_y=5$	Y39,Y111,Y120,Y121,Y140	0.0748
	Y39,Y79,Y111,Y120,Y140	0.0748
	Y111,Y115,Y120,Y121,Y140	0.0752

is very efficient and successfully identifies promising subsets when the number of measurements  $n_y \leq 6$ . However, when  $n_y = 7$  the algorithm consumes about 1 min to complete the search, and the CPU time further increases as  $n_y$  increases. Fortunately, most of the loss is reduced when  $n_y$  is small, Table 7 summarizes the obtained results when  $n_y = 2$  to 5.

When  $n_y = 2$ , the best subset is identified as Y32 (Quencher outlet flow rate) and Y111 (Furnace heat duty) with an annual loss of 2.26 k\$. The second best subset is Y34 (Separator vapor outlet flow rate) and Y111, whose annual loss is 2.41 k\$. It should be stressed that the gSOC not only solves the combination matrix, but also the optimal setpoints in the whole operating space. When only two measurements are considered, it is equivalent to controlling individual measurements. In our result, the optimal setpoints for Y32 and Y111 should be 893.7 lb mol/h and 39.57 kW, respectively. On the other hand, de Araujo et al. (2007a) identified Y51 (Mixer outlet methane mole fraction) and Y58 (Quencher outlet toluene mole fraction) based on local analysis. However, the minimal loss in this case is calculated as 5.49 k\$/year, which is twice more than our result. The optimal setpoints for Y51 and Y58 are 0.702 and 0.0134, respectively. Furthermore, when they are fixed at nominal values, the economic loss is 5.97 k\$/year. Note that the evaluated loss is different from the one shown in Table 6 (de Araujo et al., 2007a), where the difference may come from: 1. different platforms (theirs in Aspen Plus and ours in Matlab); 2. in our case, we have not considered implementation errors.

When  $n_y = 3$ , the best measurements are identified as Y35 (Separator liquid outlet flow rate), Y53 (Mixer outlet toluene mole fraction) and Y115 (Benzene column reboiler heat duty). The combination matrix is

$$\mathbf{H}_1 = \begin{bmatrix} 0.0275 & 0.0025 & 0.8023 & -0.506 \\ -0.0809 & 0.0012 & 20.87 & -0.481 \end{bmatrix}$$

where coefficients in the first column are negative optimal set-points. By calculation, the loss of  $\mathbf{H}_1$  is 0.287 k\$/year, which is one order of magnitude less than the case of  $n_y = 3$ . The second best subset is to replace Y35 as Y57 (Quencher outlet benzene mole fraction), which however leads to a much bigger loss (0.931 k\$/year).

When  $n_y = 4$ , the best subset is Y2 (FEHE hot side outlet temperature), Y35 (Separator liquid outlet flow rate), Y47

(Stabilizer distillate flow rate) and Y115 (Benzene column reboiler heat duty). The combination matrix is

$$\mathbf{H}_2 = \begin{bmatrix} 2.496 & -0.0071 & 0.0025 & 0.533 & -2.54 \\ 3.227 & -0.0074 & 0.0013 & 0.268 & -1.307 \end{bmatrix}$$

with a loss of 0.205 k\$/year, whose improvement is however not very significant compared to the case of  $n_y = 3$ . When  $n_y = 5$ , the best subset is Y39 (Benzene column boilup flow rate), Y111 (Furnace heat duty), Y120 (Stabilizer distillate to feed flow ratio), Y121 (Benzene column bottoms to feed flow ratio) and Y140 (Heavy key recovery in toluene column top (diphenyl)). The combination matrix is

$$\mathbf{H}_3 = \begin{bmatrix} 7.65 & -0.013 & 0.04 & -38.2 & -12.2 & 973.1 \\ 4.84 & -0.007 & 0.012 & -23.25 & -6.96 & 598.1 \end{bmatrix}$$

with a loss of 0.0748 k\$/year.

Based on the above results, we would finally recommend using the optimal subset in the case of  $n_y = 3$  (Y35, Y53, Y115) and  $\mathbf{H}_1$  as the combination matrix to formulating the self-optimizing CVs, such that a good trade-off is made between the economic performance and CV complexity. Compared to the previous control structure designed by de Araujo et al. (2007a), the economic profit of plant operation can be improved by about 5.7 k\$/year using this control reconfiguration.

## 6. CONCLUSIONS

In this paper, we considered control reconfiguration for the HDA plant to improve the process optimality. The methodology is based on the self-optimizing control, which has been applied to the HDA plant. However, we made further improvements using the global self-optimizing control (gSOC) approach (Ye et al., 2015) combined with the PB<sup>3</sup> algorithm (Kariwala and Cao, 2010; Ye et al., 2017).

For the HDA plant, we identify several promising alternatives for the self-optimizing control purpose. For example, the case of  $n_y = 3$  is a reasonable choice where the optimal measurements are Y35 (Separator liquid outlet flow rate), Y53 (Mixer outlet toluene mole fraction) and Y115 (Benzene column reboiler heat duty). In this case, the economic profit can be improved by 5.7 k\$/year compared to the previous result. In the future work, both the effects of implementation errors and dynamic validations can be included to further assess the obtained results.

## REFERENCES

- Alstad, V. and Skogestad, S. (2007). Null space method for selecting optimal measurement combinations as controlled variables. *Ind. Eng. Chem. Res.*, 46(3), 846–853.
- Cao, Y. (1995). *Control Structure Selection for Chemical Processes using Input-Output Controllability Analysis*. Ph.D. thesis, the University of Exeter.
- Cao, Y. and Biss, D. (1997). An Input Pre-Screening Technique for Control Structure Selection. *Computers and Chemical Engineering*, 21(6), 563–569.
- Cao, Y. and Kariwala, V. (2008). Bidirectional branch and bound for controlled variable selection: Part I. Principles and minimum singular value criterion. *Comput. Chem. Engng.*, 32(10), 2306–2319.
- Cao, Y., Rossiter, D., and Owens, D.H. (1998). Output effectiveness and scaling sensitivity for secondary measurement selection. *Transaction of IChemE, Part A*, 76, 849–854.
- de Araujo, A.C.B., Govatsmark, M., and Skogestad, S. (2007a). Application of plantwide control to the hda process. I steady-state optimization and self-optimizing control. *Control engineering practice*, 15(10), 1222–1237.
- de Araujo, A.C.B., Hori, E.S., and Skogestad, S. (2007b). Application of plantwide control to the HDA process. II Regulatory control. *Ind. Eng. Chem. Res.*, 46, 5159–5174.
- Douglas, J. (1988). *Conceptual Design of Chemical Processes*. McGRAW-Hill.
- Halvorsen, I.J., Skogestad, S., Morud, J.C., and Alstad, V. (2003). Optimal selection of controlled variables. *Ind. Eng. Chem. Res.*, 42(14), 3273–3284.
- Jäschke, J., Cao, Y., and Kariwala, V. (2017). Self-optimizing control—a survey. *Annual Reviews in Control*, 43, 199–223.
- Kariwala, V. and Cao, Y. (2009). Bidirectional branch and bound for controlled variable selection: Part II. Exact local method for self-optimizing control. *Comput. Chem. Eng.*, 33(8), 1402–1412.
- Kariwala, V. and Cao, Y. (2010). Bidirectional branch and bound for controlled variable selection: Part III. Local average loss minimization. *IEEE Trans. Ind. Informat.*, 6(1), 54–61.
- Kariwala, V., Cao, Y., and Janardhanan, S. (2008). Local self-optimizing control with average loss minimization. *Ind. Eng. Chem. Res.*, 47(4), 1150–1158.
- Luyben, W., Tyreus, B., and Luyben, M. (1999). *Plantwide Process Control*. McGraw Hill.
- Skogestad, S. (2000). Plantwide control: The search for the self-optimizing control structure. *J. Process Control*, 10(5), 487–507.
- Skogestad, S. (2004). Control structure design for complete chemical plants. *Comput. Chem. Eng.*, 28(1), 219–234.
- Ye, L. and Cao, Y. (2012). A formulation for globally optimal controlled variable selection. In *UKACC International Conference on Control*, 136–141.
- Ye, L., Cao, Y., Li, Y., and Song, Z. (2013). Approximating necessary conditions of optimality as controlled variables. *Ind. Eng. Chem. Res.*, 52(2), 798–808.
- Ye, L., Cao, Y., Ma, X., and Song, Z. (2014). A novel hierarchical control structure with controlled variable adaptation. *Ind. Eng. Chem. Res.*, 53(38), 14695–14711.
- Ye, L., Cao, Y., and Xiao, Y. (2015). Global approximation of self-optimizing controlled variables with average loss minimization. *Ind. Eng. Chem. Res.*, 54(48), 12040–12053.
- Ye, L., Cao, Y., Yuan, X., and Song, Z. (2016). Retrofit self-optimizing control of tennessee eastman process. In *Industrial Technology (ICIT), 2016 IEEE International Conference on*, 866–871. IEEE.
- Ye, L., Cao, Y., Yuan, X., and Song, Z. (2017). Retrofit self-optimizing control: A step forward toward real implementation. *IEEE Transactions on Industrial Electronics*, 64(6), 4662–4670.